
MAVIS: Mathematical Visual Instruction Tuning

Renrui Zhang^{*1}, Xinyu Wei^{*2}, Dongzhi Jiang¹, Yichi Zhang², Ziyu Guo¹
Chengzhuo Tong³, Jiaming Liu², Aojun Zhou¹, Bin Wei⁴
Shanghang Zhang², Peng Gao³, Hongsheng Li¹

¹CUHK ²Peking University ³Shanghai AI Laboratory ⁴Oracle
{renruizhang, dzjiang, ziyuguo}@link.cuhk.edu.hk

Abstract

Multi-modal Large Language Models (MLLMs) have recently emerged as a significant focus in academia and industry. Despite their proficiency in general multi-modal scenarios, the mathematical problem-solving capabilities in visual contexts remain insufficiently explored. We identify three key areas within MLLMs that need to be improved: *visual encoding of math diagrams*, *diagram-language alignment*, and *mathematical reasoning skills*. This draws forth an urgent demand for large-scale, high-quality data and training pipelines in visual mathematics. In this paper, we propose **MAVIS**, the first **MA**thematical **VIS**ual instruction tuning paradigm for MLLMs, involving a series of mathematical visual datasets and specialized MLLMs. Targeting the three issues, MAVIS contains three progressive training stages from scratch. First, we curate **MAVIS-Caption**, consisting of 558K diagram-caption pairs, to fine-tune a math-specific vision encoder (CLIP-Math) through contrastive learning, tailored for improved diagram visual encoding. Second, we utilize MAVIS-Caption to align the CLIP-Math with a large language model (LLM) by a projection layer, enhancing vision-language alignment in mathematical domains. Third, we introduce **MAVIS-Instruct**, including 900K meticulously collected and annotated visual math problems, which is adopted to finally instruct-tune the MLLM for robust mathematical reasoning skills. In MAVIS-Instruct, we incorporate complete chain-of-thought (CoT) rationales for each problem, and minimize textual redundancy, thereby concentrating the model towards the visual elements. Note that both our new datasets span a broad range of math subjects to ensure comprehensive capabilities, including plane geometry, analytic geometry, and function. On various mathematical benchmarks, e.g., MathVerse, MAVIS-7B achieves leading performance among open-source MLLMs, surpassing other 7B models by +11.0% and the second-best LLaVA-NeXT (110B) by +3.0%, demonstrating the effectiveness of our approach. Data and Models are released at <https://github.com/ZrrSkywalker/MAVIS>.

1 Introduction

The pursuit of artificial general intelligence (AGI) necessitates models to seamlessly integrate, interpret, and generate multi-modal data. In recent years, the advent of Large-language Models (LLMs) [5, 28, 58, 59, 16] and their Multi-modal extension (MLLMs) [70, 20, 55, 13, 64] have significantly facilitated this process across various fields, such as healthcare [54, 53, 69], autonomous driving [63, 29], and robotics [36, 42]. Although MLLMs exhibit remarkable performance in diverse tasks and benchmarks, one arena where they have yet to fully demonstrate their potential is mathematical problem-solving in visual contexts.

*Equal Contribution

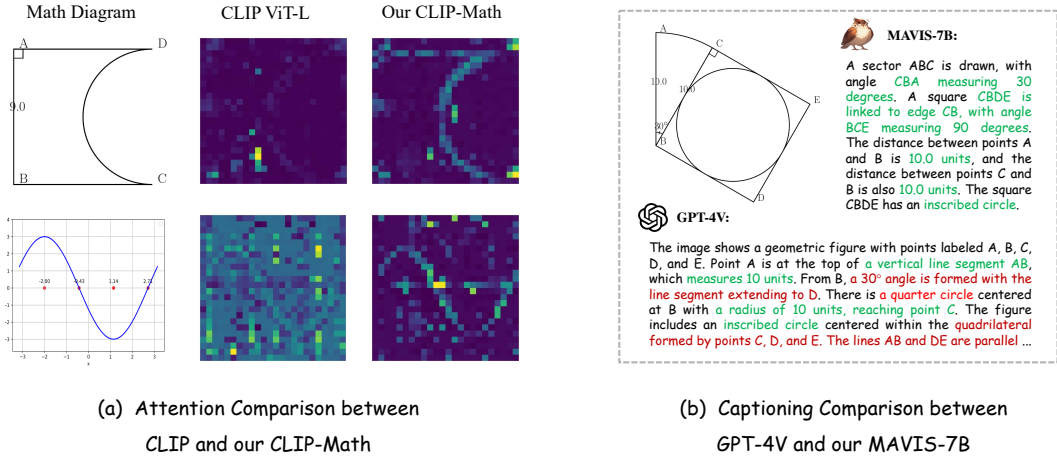


Figure 1: (a) We compare the attention map of class tokens from CLIP ViT-L [51] and our CLIP-Math. Our vision encoder can better capture significant mathematical information within diagrams. (b) We compare the diagram captioning capabilities between GPT-4V [49] and our MAVIS-7B, where GPT-4V fall short of accurately recognizing mathematical visual elements.

Existing efforts [48, 47, 72] for text-only mathematics have attained considerable progress, attributed to the sufficient training data and inherent language proficiency within LLMs. However, visual mathematical problem-solving poses unique challenges for MLLMs, requiring them to integrate the analytical depth of textual questions with the contextual richness of visual diagrams. We observe three critical issues that severely hinder the visual mathematical capabilities of MLLMs.

- i. **Unsatisfactory math diagram embeddings by vision encoders.** Most MLLMs adopt a frozen CLIP [51] as the vision encoder, which is pre-trained by natural images capturing real-world scenes with rich colors and textures. In contrast, math diagrams are composed of abstract curves, shapes, and symbols with a monochromatic color scheme, exhibiting large semantic gaps to general scenarios. As visualized in Figure 1 (a), the attention map of CLIP struggles to capture important information within math diagrams, which cannot provide satisfactory visual embeddings for LLMs to understand.
- ii. **Diagram-language misalignment between vision encoders and LLMs.** Likewise, the vision-language pre-training stage of MLLMs also adopts natural image-caption pairs for cross-modal alignment. Due to the domain gap, while they can generate accurate captions for real-world images, but fall short of recognizing basic mathematical elements and narrating their relations. As compared in Figure 1 (b), even GPT-4V [49] produces low-quality descriptions for simple geometric figures and functions, indicating LLMs are not well aligned with the visual embedding space of math diagrams.
- iii. **Inaccurate mathematical reasoning with visual elements by MLLMs.** Referring to MathVerse [71], incorporating the diagram input would adversely affect the reasoning quality of MLLMs compared to using only the text-only question. From their demonstrations, we observe the problem-solving process of GPT-4V and Gemini-Pro [22] both suffer from low-quality chain-of-thought (CoT) reasoning accuracy. This demonstrates the incapability of MLLMs to leverage visual cues for precise mathematical problem-solving.

Therefore, to mitigate these issues, it is essential to develop an extensive dataset and effective training approach tailored to visual mathematics. In this paper, we propose **MAVIS**, the first **MA**thematical **VIS**ual instruction tuning paradigm for MLLMs, which aims to fully unleash their potential for diagram visual encoding and reasoning capabilities. We introduce two meticulously curated datasets, a progressive three-stage training pipeline, and a visual mathematical specialist, MAVIS-7B. We summarize the contributions of our work as follows.

- **MAVIS-Caption & MAVIS-Instruct.** We curate two large-scale, high-quality mathematical visual datasets, widely covering plane geometry, analytic geometry, and function. MAVIS-Caption consists of 558K diagram-caption pairs, which are automatically created by a delicately designed data engine with accurate vision-language correspondence. MAVIS-

Instruct includes 834K visual math problems, which are obtained from four sources: 83k augmented by GPT-4V from manually collected 4K problems, 51K generated by GPT-4V based on diagram-caption pairs, 117k augmented from existing datasets, and 582K directly constructed by our data engine. Each problem is annotated with a CoT rationale, and modified to contain minimized textual redundancy for more informative visual diagrams.

- **Three-stage Training Pipeline.** Our training framework involves three progressive stages designed to sequentially address the aforementioned identified deficiencies in MLLMs. Firstly, we utilize MAVIS-Caption to fine-tune a math-specific vision encoder by contrastive learning, termed CLIP-Math, to enable better visual representations of math diagrams. Subsequently, we align this encoder with the LLM to ensure effective diagram-language integration also by MAVIS-Caption. Finally, our MAVIS-Instruct is adopted to instruction-tune the MLLM. The annotated CoT rationale can provide sufficient supervision for the intricate reasoning capabilities, and the vision-dominant format can better focus models on leveraging visual inputs.
- **Mathematical Visual Specialist.** After the three-stage training, we develop MAVIS-7B, an MLLM specifically optimized for visual mathematical problem-solving. On various evaluation benchmarks, our model achieves leading performance compared to existing open-source MLLMs, e.g., surpassing other 7B models by +11.0% and the second-best LLaVA-NeXT (110B) [31] by +3.0% on the average accuracy of MathVerse [71]. The quantitative results and qualitative analysis both validate the significance of our approach.

2 Related Work

Visual Instruction Tuning. The advancement of large language models (LLMs) [5, 28, 59, 16] with instruction tuning has significantly enhanced zero-shot capabilities across a range of tasks. Drawing inspiration from this, LLaMA-Adapter series [70, 20, 26] propose a zero-initialized attention mechanism to align frozen vision encoders [51] with LLaMA [58] for multi-modal learning. LLaVA series [41, 39] employ a linear projector for vision-language alignment, establishing visual instruction tuning as a standard training approach in the multi-modal field. Flamingo [2] and OpenFlamingo [3] have honed visual representation by integrating a cross-attention resampler with vision encoders. SPHINX series [21, 38] utilize a blend of visual encoders to make the LLM cognizant of various image aspects. InternVL series [15, 17, 56] employ a large vision encoder and QFormer [34] to incorporate high-quality visual information through a multi-stage training methodology. LLaVA-NexT [40, 31, 33] further introduces the ‘AnyRes’ technique to manage images at any given resolution, and LLaVA-NexT-Interleave [32] extends the scope widely to interleave multi-image settings. There are also recent efforts to apply visual instruction tuning to 3D [25, 62] and video [35, 18] scenarios. Despite the impressive strides made in both model capability and training efficiency by multi-modal large language models (MLLMs) through visual instruction tuning, there is currently no MLLM specifically designed for mathematical problem-solving, nor a substantial dataset available for such purposes in the open-source community. In this paper, we mitigate the issue by proposing MAVIS with high-quality mathematical visual datasets and training paradigms.

Mathematics in Large Models. Recent research has predominantly concentrated on text-only mathematical problem-solving using LLMs. MAMmoTH [67, 68] have compiled extensive collections of mathematical problems, training LLMs using the reasoning processes described in solutions. MetaMATH [66] has expanded upon this by rewriting existing problems to create a larger dataset. MathCoder [60] and ToRA [24] introduced a tools agent approach, employing Python code and symbolic resolvers during the training phase, significantly outperforming traditional models that rely on text-only mathematical reasoning. However, in the multi-modal field, despite the introduction of several datasets such as Geometry3K [44], GeoQA [11], UniGeo [8], UniMath [37], and GeomVerse [30], aiming at enhancing the performance of MLLMs in solving graphical mathematical problems, these datasets are quite limited in scale and domain. Based on these datasets, G-LLaVA [19] has developed superior capabilities for understanding graphical geometries but struggles with mathematical problems in other domains. The comprehensive benchmark MathVerse [71] has also highlighted the existing MLLMs’ unsatisfactory capacity for encoding visual diagrams in diverse mathematical domains. Therefore, there is a pressing need for the development of more robust encoders for mathematical images and the tuning of MLLMs with mathematical visual instructions, for which we propose MAVIS to address the challenges.

Table 1: Statistics of MAVIS-Caption.

Statistic	Number
<i>Total Captions</i>	
- Total number	588K
- Average length (words)	62.85
- Average length (characters)	339.68
- Vocabulary size	418
<i>Plane Geometry</i>	
- Total number	299K (50.9%)
- Average length (words)	69.77
- Average length (characters)	385.85
- Vocabulary size	195
<i>Analytic Geometry</i>	
- Total number	77K (13.1%)
- Average length (words)	39.64
- Average length (characters)	210.10
- Vocabulary size	158
<i>Function</i>	
- Total number	212K (36.0%)
- Average length (words)	61.48
- Average length (characters)	321.46
- Vocabulary size	149

Table 2: Subject Distribution of MAVIS-Instruct.

Statistic	Number
<i>Total questions</i>	
- Multiple-choice questions	615K (62.4%)
- Free-form questions	218K (37.6%)
<i>Manual Collection Augmented by GPT-4</i>	
- Geometry questions	72K (86.5%)
- Function questions	11K (13.5%)
<i>Existing Datasets Augmented by GPT-4</i>	
- Geometry questions	117K (100.0%)
- Function questions	0 (0%)
<i>Data Engine Captions Annotated by GPT-4</i>	
- Geometry questions	30K (58.8%)
- Function questions	21K (41.2%)
<i>Data Engine Generated Problems</i>	
- Geometry questions	466K (80.0%)
- Function questions	116K (20.0%)
Number of unique images	611K (73.3%)
Number of unique questions	804K (96.5%)
Number of unique answers	675K (81.0%)
Average question length	44.60
Average answer length	62.82

3 Mathematical Visual Dataset

In Section 3.1, we first illustrate the methodology of our data engine to automatically generate math diagrams. Then, we respectively introduce the two datasets we newly curated for MLLMs, i.e., MAVIS-Caption in Section 3.2 and MAVIS-Instruct in Section 3.3.

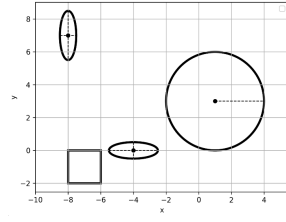
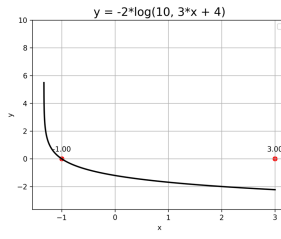
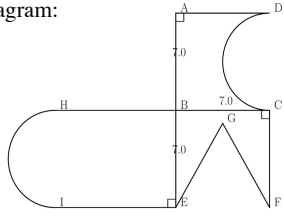
3.1 Data Engine

To cope with the substantial data requirements of MLLMs, it is essential to have access to hundreds of thousands of training instances. However, for visual mathematics, the paucity of publicly available datasets poses a challenge, and creating such data manually is also not feasible due to the high cost involved. Therefore, we develop an automatic data engine to generate high-quality math diagrams efficiently, as showcased in Figure 1. Covering most mathematical scenarios, we adopt three diagram types: plane geometry, analytic geometry, and function. Note that all the logic of the data engine is implemented in Python, and we employ Matplotlib for the graphical rendering of the diagrams.

Plane Geometry Diagram. As such diagrams typically consist of spatial combinations of various basic shapes, we utilize principles from multi-hop data curation to develop customized generation rules. These rules allow for the iterative integration of new shapes into existing configurations. Initially, we establish a core set of shapes, including squares, rectangles, triangles, sectors, etc, for diagram generation. Starting with a randomly selected shape, we extend another shape from the set along one of its straight sides. By iterating this process, we can construct diverse plane geometry diagrams featuring different combinations of shapes. Additionally, we randomly label the vertices with letters (e.g., A, B, C) and annotate numerical values relevant to geometric properties (e.g., side lengths and angles), simulating realistic plane geometry problems.

Analytic Geometry Diagram. Likewise, our approach begins by defining a basic figure set that differs slightly from that used in plane geometry; for example, we include additional elements such as points and line segments. We then construct a Cartesian coordinate system, complete with grid lines and scaled axes. The range of the coordinate system is randomly determined within a predefined scope. Subsequently, we select a number from 1 to 3 to indicate the number of figures to be drawn on the graph, and randomly choose coordinates for the top-left vertices to plot these figures at varied sizes (using these points as centers for circles). Unlike plane geometry, we ensure that the figures do not overlap, except for points and segments, and maintain the figure areas within a suitable scale.

Diagram:



Caption:

A rectangle ABCD has a semicircle inscribed using CD as the diameter, and CD is removed. Connected to edge CB is a modified rectangle CBEF,Connected to edge EB is rectangle EBHI with a semicircle outside using HI as the diameter, and side HI is eliminated. The lengths of AB, CB, EB are each 7.0 units.

The expression for the function is $y = -2 \cdot \log(10, 3 \cdot x + 4)$. When examining the x range of $[-4.0, 3.0]$, zero points appear at -1.0 . In the range $[-4.0, 3.0]$, while the function reaches its minimum value of -2.23 at 3.0 , it does not have a maximum value point. An asymptote of the function is observed at: $x = -1.33$.

At the outset, A circle with a center at $(1, 3)$ and radius 3 is present. Consequently, A rectangle originates from its lower left corner at $(-8, -2)$ and has a height of 2 and a width of 2 . Also, Located at $(-8, 7)$, At $(-4, 0)$, there is an ellipse with dimensions: height 1 and width 3 .

Figure 2: **MAVIS-Caption Dataset.** We showcase three diagram-caption pairs of plane geometry, function, and analytic geometry in MAVIS-Caption, generated by our developed data engine.

Function Diagram. We focus on seven fundamental function types: polynomial, sine, cosine, tangent, logarithmic, absolute value, and piece-wise polynomial functions. For each function type, we parameterize the equations with random variables, such as coefficients and constants within a predefined range (e.g., a and b in $y = ax + b$), which facilitates the generation of diverse function graphs. We also adopt the same Cartesian coordinate system employed for analytic geometry. Additionally, for specific caption or question-answering samples, we also plot key features like extreme points and zero points of the functions, providing additional visual information that aids in the understanding and reasoning of these mathematical functions.

3.2 MAVIS-Caption

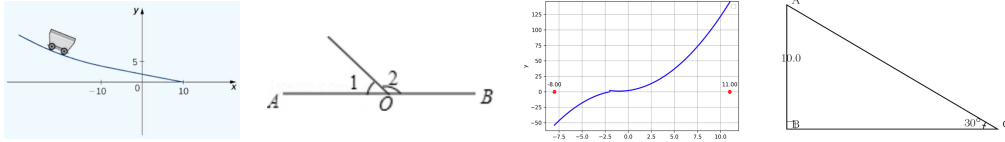
With our mathematical visual data engine, we first curate a diagram-caption dataset, MAVIS-Caption, as shown in Figure 2, aiming to benefit the diagram visual representations and cross-modal alignment.

Data Overview. As presented in Table 1, the MAVIS-Caption dataset comprises 588K diagram-caption pairs. This includes 299K for plane geometry, 77K for analytic geometry, and 212K for function. The average word length of the captions is 61.48 words, reflecting their detailed descriptive nature. The overall vocabulary size is 149, indicating the diversity in language expression.

Caption Annotation. We adopt different strategies to generate captions for three types of diagrams. Note that all the curated captions are refined by ChatGPT [50] at last for a human-like expression.

- **Plane Geometry Caption.** We follow the iterative geometric generation process to develop regulations for an accurate and detailed caption. We first prompt GPT-4 [48] to create three sets of language templates: the descriptive content for fundamental shapes (e.g., “A *Triangle* {} with two congruent sides {} and {}”), the phrases to denote specific attributes (e.g., “Angle {} measures {} degrees”), and the conjunction to link two adjacent shapes (e.g., “Attached to edge {} of shape {}, there is a {}”). Then, based on various generation scenarios, we fill and merge these templates to acquire a coherent description of the geometric figure.
- **Analytic Geometry Caption.** We also employ GPT-4 to obtain two sets of language templates: the description of coordinates and attribute information for basic figures (e.g., “The square with its base left corner at {} features sides of {} in length”) and the spatial relation for nearby figures (e.g., “On the bottom right of {}, there is a {}”). The captions are then formulated by filling in the coordinates and selecting appropriate spatial relationship templates through coordinate comparison.
- **Function Caption.** As function diagrams typically showcase a single curve, we directly utilize GPT-4 to generate templates describing various properties of functions, including expressions, domains, ranges, extreme points, and zero points. Each template is then filled based on specific cases, such as “The expression of the function is $y = -3x^3 - 2x^2 - 2x - 2$. Within the range of x values $[-3.0, 4.0]$, zero points occur at -0.83 ...”.

Diagram:



Question & Rationale:

<p>A toy company wants to design a track for a toy car that starts out along a parabolic curve and then converts to a straight line. The function that describes the track is to have the form $f(x) = ax^2 + bx + c$. Find values of b and c that make $f(x)$ both continuous and differentiable.</p>	<p>In the given diagram, if angle 1 has a measure of 35°, what is the measure of angle 2?</p> <p>A: 55 B: 135 C: 145 D: 155</p>	<p>What shape does the graph resemble in the segment x in $[-2, 11]$?</p> <p>A. V-shape; B. declining parabola; C. rising parabola; D. straight line</p>	<p>What is the length of slope AC?</p>
<p>$b = 7/4$ $c = 10 * (7/4) - 5 = 25/2$</p>	<p>Since angle 1 + angle 2 = 180°, and angle 1 = 35°, therefore angle 2 = 145°. Therefore, option C is selected.</p>	<p>The graph section from -2 to 11 shows a consistently rising curve, which demonstrates the characteristics of a quadratic function with a positive leading coefficient. So the answer is C.</p>	<p>Given $AB = 10$ units, Angle $C = 30$ degree, $AB = AC * \sin(30) = AC * 0.5$, thus $AC = AB * 2 = 20$ units</p>

Manual Collection
Augmented by GPT-4

Existing Datasets
Augmented by GPT-4

Data Engine
Generated Problems

Data Engine
Generated Problems

Figure 3: **MAVIS-Instruct Dataset**. We showcase the generated visual math problems from four sources within MAVIS-Instruct, which contain detailed rationales and minimized textual redundancy.

3.3 MAVIS-Instruct

Besides the diagram-caption data for cross-modal alignment, we curate MAVIS-Instruct of extensive problem-solving data to endow MLLMs with visual mathematical reasoning capabilities, as shown in Figure 3.

Data Overview. As illustrated in Table 2, the MAVIS-Instruct dataset consists of a total of 834K visual math problems. Given that the proportion of analytic geometry problems is relatively small, we classify them with function problems for simplicity. Each problem in MAVIS-Instruct includes a CoT rationale providing step-by-step solutions, with an average answer length of 150 words. We have minimized textual redundancy in the questions, eliminating unnecessary contextual information, distracting conditions, and attributes readily observable from the diagrams. This reduction in text forces MLLMs to enhance their capability to extract essential content from visual inputs. MAVIS-Instruct is assembled from four distinct sources to ensure broad coverage.

Manual Collection Augmented by GPT-4. To incorporate high-quality problems found in real-world contexts, we manually collect 4K math problems with diagrams from publicly available resources. Recognizing that these sources often lack detailed rationales and may contain redundant text, we initially utilize GPT-4V to annotate a detailed solving process and streamline the question text to reduce redundancy. Subsequently, for each collected instance, we input the question, rationale, and diagram into GPT-4 and employ customized few-shot prompts to generate 20 new problems per original, comprising 15 multiple-choice questions and 5 free-form questions. This process contributes a total of 84K problems to the dataset.

Existing Datasets Augmented by GPT-4. Given existing well-organized geometric datasets, we can also leverage them to expand MAVIS-Instruct. Referring to previous prompt designs, we augment the 8K training set from two dataset, Geometry-3K and GeoQA+, into 80K visual problems with accompanying rationales, mapping each original problem to 10 new ones. Due to the scarcity of publicly available function data, we do not include function problems from this source.

Data Engine Captions Annotated by GPT-4. Given the detailed captions and diagrams generated by our data engine, we can prompt GPT-4V with these sufficient conditions to generate accurate question-answering data. We first generate a new set of 17K diagram-caption pairs that do not overlap with the previous MAVIS-Caption, which avoids answer leakage within the detailed caption. Then, we prompt GPT-4V to generate 3 new problems with rationales, obtaining 51K data in total from the diagram-caption pairs.

Data Engine Generated Problems. In addition to relying on GPT for data generation, we manually craft rigorous regulations to produce visual math problems directly from our data engine.

- **Plane Geometry Problems.** We initially prompt GPT-4 to compile a comprehensive set of mathematical formulas applicable to each basic shape (e.g., Pythagorean theorem for right triangles and area formula for circles). Then, for a geometric diagram, we randomly select a known condition within a shape as the final solution target, and systematically deduce backward to another condition, either within the same shape or an adjacent one, using a randomly selected mathematical formula. This deduced condition is then set as unknown, and we continue iterative backward deductions as necessary. The final condition, along with any conditions in the last step, are presented as initial attributes in the question. The rationales can be simply obtained by reversing this backward deduction process.
- **Function Problems.** As the properties of functions are predetermined, we utilize GPT-4 to generate diverse reasoning templates. These templates facilitate the solving of one function property based on other provided properties, thereby ensuring the generation of high-quality function rationales. We finally obtain 299K plane geometry and 212K function problems.

4 Mathematical Visual Training

With the curated datasets, we devise a three-stage training pipeline for endowing MLLMs with mathematical visual capabilities. They respectively aim to mitigate the three deficiencies within existing MLLMs, i.e., diagram visual encoding, diagram-language alignment, and mathematical reasoning skills in visual contexts.

4.1 Stage 1: Training CLIP-Math

To enhance CLIP’s [51] inadequate visual encoding of math diagrams, we utilize MAVIS-Caption to train a specialized CLIP-Math encoder. Specifically, we fine-tune a pre-trained CLIP-Base model following the conservative learning scheme. The math diagrams are fed into the learnable vision encoder, while the corresponding captions are processed by the text encoder, which remains frozen to provide reliable supervision. Via contrastive training, the model learns to adapt from its original natural image domain to mathematical contexts, increasing its focus on essential visual elements within diagrams, as demonstrated in Figure 1 (a). The optimized CLIP-Math encoder now delivers more precise and robust representations of math diagrams, establishing a solid foundation for the subsequent visual interpretation of LLMs.

4.2 Stage 2: Aligning Diagram-language

After acquiring the CLIP-Math encoder, we further integrate it with LLMs using MAVIS-Caption to boost cross-modal alignment between math diagrams and language embedding space. Using a simple two-layer MLP as the projection layer, we transform the visual encodings from CLIP-Math, and prepend them as a prefix to the LLM input. This process, guided by the diagram captioning task, enables the LLM to accurately recognize mathematical components and describe their spatial arrangements. With the diagram-language alignment, LLMs are equipped with the interpretation capability in math diagrams, serving as an initial step toward deeper mathematical reasoning. In this stage, we freeze the CLIP-Math, and train the projection layer along with the LoRA-based [27] LLM.

4.3 Stage 3: Instruction Tuning

Lastly, we leverage MAVIS-Instruct to endow MLLMs with CoT reasoning and problem-solving capabilities in visual mathematics. The detailed rationales within each problem’s solution provide high-quality reasoning guidance for MLLMs, significantly enhancing their step-by-step CoT process. Furthermore, the adopted text-lite, vision-dominant, and vision-only problem formats facilitate MLLMs to capture more essential information from the visual embeddings for problem-solving, rather than relying on shortcuts to only process the textual content within questions. During this stage, we unfreeze both the projection layer and the LoRA [27]-based LLM to perform a thorough instruction-following tuning, which finally results in MAVIS-7B.

Table 3: **Performance Comparison on MathVerse** with the accuracy metric. The highest results for closed-source and open-source MLLMs are marked in red and blue respectively.

Model	Base LLM	All	Text Dominant	Text Lite	Vision Intensive	Vision Dominant	Vision Only
		Acc	Acc	Acc	Acc	Acc	Acc
<i>Baselines</i>							
Random Chance	-	12.4	12.4	12.4	12.4	12.4	12.4
Human	-	67.7	71.2	70.9	61.4	68.3	66.7
<i>LLMs</i>							
ChatGPT [50]	-	26.1	33.3	18.9	-	-	-
GPT-4 [48]	-	33.6	46.5	46.5	-	-	-
<i>Closed-source MLLMs</i>							
Qwen-VL-Plus [4]	-	11.8	15.7	11.1	9.0	13.0	10.0
Gemini-Pro [22]	-	23.5	26.3	23.5	23.0	22.3	22.2
Qwen-VL-Max [4]	-	25.3	30.7	26.1	24.1	24.1	21.4
GPT-4V [49]	-	39.4	54.7	41.4	34.9	34.4	31.6
<i>Open-source MLLMs</i>							
LLaMA-Adapter V2 [20]	LLaMA-7B [58]	5.8	7.8	6.3	6.2	4.5	4.4
ImageBind-LLM [26]	LLaMA-7B	10.0	13.2	11.6	9.8	11.8	3.5
mPLUG-Owl2 [65]	LLaMA-7B	10.3	11.6	11.4	11.1	9.4	8.0
MiniGPT-v2 [13]	LLaMA2-7B [59]	10.9	13.2	12.7	11.1	11.3	6.4
SPHINX-Plus [21]	LLaMA2-13B	14.0	16.3	12.8	12.9	14.7	13.2
SPHINX-MoE [21]	Mixtral-8×7B [28]	15.0	22.2	16.4	14.8	12.6	9.1
G-LLaVA [19]	LLaMA2-7B	15.7	22.2	20.4	16.5	12.7	6.6
InternLM-XC2. [17]	InternLM2-7B [6]	16.5	22.3	17.0	15.7	16.4	11.0
LLaVA-1.5 [39]	Vicuna-13B	17.0	18.7	18.5	18.1	16.1	13.8
ShareGPT4V [14]	Vicuna-13B	17.4	21.8	20.6	18.6	16.2	9.7
Math-LLaVA [52]	Vicuna-13B	19.0	21.2	19.8	20.2	17.6	16.4
LLaVA-NeXT [31]	LLaMA3-8B [57]	19.3	24.9	20.9	20.8	16.1	13.8
LLaVA-NeXT	Qwen-1.5-110B [1]	24.5	31.7	24.1	24.0	22.1	20.7
MAVIS-7B	MAmmoTH2-7B [68]	27.5	41.4	29.1	27.4	24.9	14.6

5 Experiment

We first detail our experimental settings in Section 5.1, and then discuss the quantitative on different benchmarks and qualitative examples in Sections 5.2 and 5.3, respectively. Please refer to the Supplementary Material for more experiments, analysis, and ablation studies.

5.1 Experimental Settings

Implementation Details. We adopt a CLIP ViT-L [51] as the pre-trained model to fine-tune our CLIP-Math, and utilize Mammoth2-7B [68] as the base LLM to construct MAVIS-7B. In the first stage, we fine-tune the CLIP for 10 epochs with a batch size 16 and an initial learning rate $2e^{-6}$. In the second stage, we train the diagram-language alignment for 1 epoch with a batch size 32 and an initial learning rate $2e^{-6}$, and adopt LoRA [27] with a rank 128. In the third stage, we adopt the same training settings as the previous one.

Evaluation Benchmarks. We evaluate our model MAVIS-7B on three popular mathematical benchmarks, MathVerse [71], GeoQA [12], and FunctionQA (a subset of function problems in MathVista [43]). MathVerse is a comprehensive benchmark containing 2.6K visual math problems spanning plane geometry, function, and solid geometry. GeoQA and FunctionQA respectively focus on plane geometry and function scenarios. We adopt the accuracy metric for all the benchmarks.

5.2 Quantitative Performance

As shown in Table 3 for the results on MathVerse, MAVIS-7B achieves the best overall accuracy among existing open-source models with only a 7B size. On different problem versions, our

Table 4: Comparison of model performance with traditional methods on **GeoQA**.

Model	Accuracy (%)
Random Chance	25.0
Frequent Guesses	32.1
<i>Top-10 Accuracy</i>	
NGS [10]	56.9
DPE-GPS [7]	62.7
SCA-GPS [45]	64.1
<i>Top-1 Accuracy</i>	
Geoformer [9]	46.8
UniMath [37]	50.0
G-LLaVA-7B [19]	64.2
MAVIS-7B	66.7

Table 5: Comparison of model performance with methods on **FunctionQA of MathVista**.

Model	Accuracy (%)
Random Chance	22.5
<i>Closed-source MLLMs</i>	
CoT GPT-4 [48]	35.0
PoT GPT-4 [48]	37.0
Multimodal Bard [23]	45.5
GPT-4V [49]	69.5
<i>Open-source MLLMs</i>	
LLaVA [41]	20.5
LLaMA-Adapter V2 [20]	32.0
LLaVA-NeXT [40]	33.7
SPHINX-MoE [21]	34.6
MAVIS-7B	40.3

approach consistently surpasses the second-best method, especially for Text Dominant and Text Lite. Specifically, our model exceeds InternLM-XComposer2 (7B) [17] by +11.0% and ShareGPT4V (13B) [14] by +10.1%. Compared to other mathematical MLLMs, i.e., G-LLaVA [19] and concurrent Math-LLaVA [52], MAVIS-7B exhibits superior problem-solving capabilities with higher scores of +11.8% and +8.5%, respectively. In addition, our model is also advantageous to the most powerful open-source MLLM series, LLaVA-NeXT [31], from 7B to 110B model sizes, demonstrating the math-specific proficiency of MAVIS-7B. Tables 4 and 5 respectively showcase our performance on plane geometry and function scenarios. Compared to those specialist models, e.g., G-LLaVA, our MAVIS-7B exhibits superior reasoning and generalization capabilities.

5.3 Qualitative Analysis

In Figure 4, we compare the mathematical problem-solving examples between MAVIS-7B and GPT-4V [49]. Our model excels in understanding the geometric elements, function curves, and coordinate axes in mathematical diagrams, achieving higher-quality CoT reasoning capabilities.

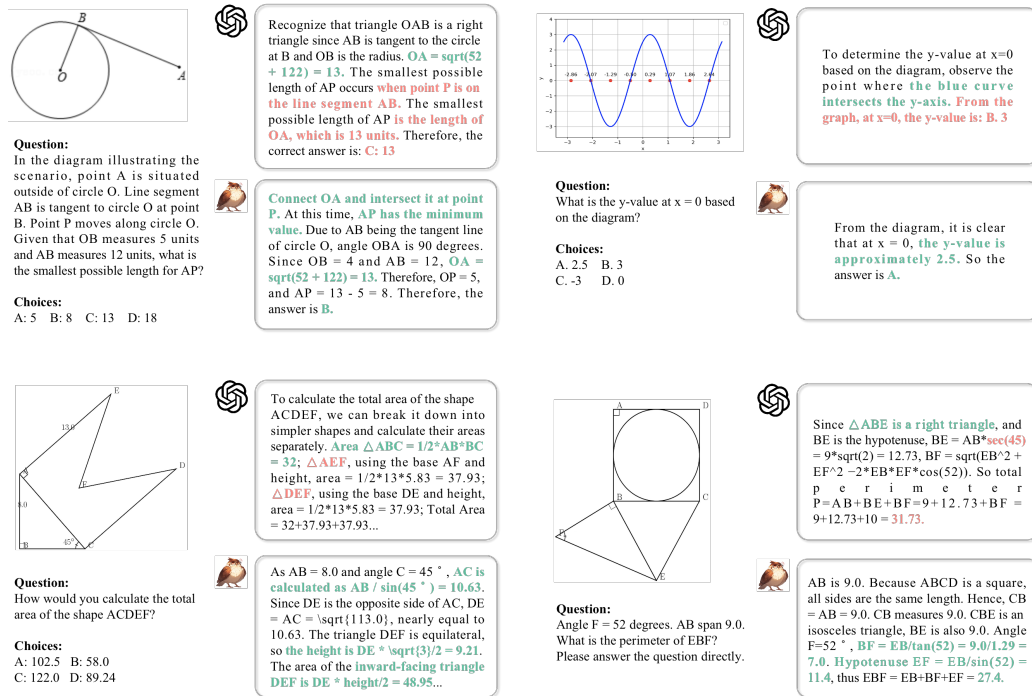


Figure 4: Problem-solving Comparison of MAVIS-7B and GPT-4V.

6 Conclusion

In this paper, we propose MAVIS, the first mathematical visual instruction tuning paradigm for MLLMs. We first introduce two high-quality datasets by a delicate data engine, MAVIS-Caption and MAVIS-Instruct, containing large-scale diagram-language and problem-solving data. Then, we customize a three-stage training framework to progressively train the math-specific vision encoder, the diagram-language alignment, and the mathematical reasoning capabilities of MLLMs. The obtained specialist model, MAVIS-7B, achieves superior performance across different mathematical visual benchmarks, demonstrating the potential to serve as a new standard for future research.

References

- [1] AI@Meta: Llama 3 model card (2024), https://github.com/meta-llama/llama3/blob/main/MODEL_CARD.md
- [2] Alayrac, J.B., Donahue, J., Luc, P., Miech, A., Barr, I., Hasson, Y., Lenc, K., Mensch, A., Millican, K., Reynolds, M., et al.: Flamingo: a visual language model for few-shot learning. *Advances in Neural Information Processing Systems* **35**, 23716–23736 (2022)
- [3] Awadalla, A., Gao, I., Gardner, J., Hessel, J., Hanafy, Y., Zhu, W., Marathe, K., Bitton, Y., Gadre, S., Sagawa, S., et al.: Openflamingo: An open-source framework for training large autoregressive vision-language models. *arXiv preprint arXiv:2308.01390* (2023)
- [4] Bai, J., Bai, S., Yang, S., Wang, S., Tan, S., Wang, P., Lin, J., Zhou, C., Zhou, J.: Qwen-vl: A versatile vision-language model for understanding, localization, text reading, and beyond. *arXiv preprint arXiv:2308.12966* (2023)
- [5] Brown, T., Mann, B., Ryder, N., Subbiah, M., Kaplan, J.D., Dhariwal, P., Neelakantan, A., Shyam, P., Sastry, G., Askell, A., et al.: Language models are few-shot learners. In: *Advances in neural information processing systems*. pp. 1877–1901 (2020)
- [6] Cai, Z., Cao, M., Chen, H., Chen, K., Chen, K., Chen, X., Chen, X., Chen, Z., Chen, Z., Chu, P., et al.: Internlm2 technical report. *arXiv preprint arXiv:2403.17297* (2024)
- [7] Cao, J., Xiao, J.: An augmented benchmark dataset for geometric question answering through dual parallel text encoding. In: *Proceedings of the 29th International Conference on Computational Linguistics*. pp. 1511–1520 (2022)
- [8] Chen, J., Li, T., Qin, J., Lu, P., Lin, L., Chen, C., Liang, X.: Unigeo: Unifying geometry logical reasoning via reformulating mathematical expression. *ArXiv* **abs/2212.02746** (2022)
- [9] Chen, J., Li, T., Qin, J., Lu, P., Lin, L., Chen, C., Liang, X.: UniGeo: Unifying geometry logical reasoning via reformulating mathematical expression. In: *Proceedings of the 2022 Conference on Empirical Methods in Natural Language Processing*. pp. 3313–3323 (2022)
- [10] Chen, J., Tang, J., Qin, J., Liang, X., Liu, L., Xing, E., Lin, L.: GeoQA: A geometric question answering benchmark towards multimodal numerical reasoning. In: Zong, C., Xia, F., Li, W., Navigli, R. (eds.) *Findings of the Association for Computational Linguistics: ACL-IJCNLP 2021*. pp. 513–523. Association for Computational Linguistics, Online (Aug 2021). <https://doi.org/10.18653/v1/2021.findings-acl.46>, <https://aclanthology.org/2021.findings-acl.46>
- [11] Chen, J., Tang, J., Qin, J., Liang, X., Liu, L., Xing, E.P., Lin, L.: Geoqa: A geometric question answering benchmark towards multimodal numerical reasoning. *ArXiv* **abs/2105.14517** (2021), <https://api.semanticscholar.org/CorpusID:235253782>
- [12] Chen, J., Tang, J., Qin, J., Liang, X., Liu, L., Xing, E.P., Lin, L.: Geoqa: A geometric question answering benchmark towards multimodal numerical reasoning. *arXiv preprint arXiv:2105.14517* (2021)
- [13] Chen, J., Li, D.Z.X.S.X., Zhang, Z.L.P., Xiong, R.K.V.C.Y., Elhoseiny, M.: Minigt-v2: Large language model as a unified interface for vision-language multi-task learning. *arXiv preprint arXiv:2310.09478* (2023)

- [14] Chen, L., Li, J., wen Dong, X., Zhang, P., He, C., Wang, J., Zhao, F., Lin, D.: Sharegpt4v: Improving large multi-modal models with better captions. ArXiv **abs/2311.12793** (2023), <https://api.semanticscholar.org/CorpusID:265308687>
- [15] Chen, Z., Wang, W., Tian, H., Ye, S., Gao, Z., Cui, E., Tong, W., Hu, K., Luo, J., Ma, Z., et al.: How far are we to gpt-4v? closing the gap to commercial multimodal models with open-source suites. arXiv preprint arXiv:2404.16821 (2024)
- [16] Chiang, W.L., Li, Z., Lin, Z., Sheng, Y., Wu, Z., Zhang, H., Zheng, L., Zhuang, S., Zhuang, Y., Gonzalez, J.E., Stoica, I., Xing, E.P.: Vicuna: An open-source chatbot impressing gpt-4 with 90%* chatgpt quality. <https://lmsys.org/blog/2023-03-30-vicuna/> (March 2023)
- [17] Dong, X., Zhang, P., Zang, Y., Cao, Y., Wang, B., Ouyang, L., Wei, X., Zhang, S., Duan, H., Cao, M., et al.: Internlm-xcomposer2: Mastering free-form text-image composition and comprehension in vision-language large model. arXiv preprint arXiv:2401.16420 (2024)
- [18] Fu, C., Dai, Y., Luo, Y., Li, L., Ren, S., Zhang, R., Wang, Z., Zhou, C., Shen, Y., Zhang, M., et al.: Video-mme: The first-ever comprehensive evaluation benchmark of multi-modal llms in video analysis. arXiv preprint arXiv:2405.21075 (2024)
- [19] Gao, J., Pi, R., Zhang, J., Ye, J., Zhong, W., Wang, Y., Hong, L., Han, J., Xu, H., Li, Z., et al.: G-llava: Solving geometric problem with multi-modal large language model. arXiv preprint arXiv:2312.11370 (2023)
- [20] Gao, P., Han, J., Zhang, R., Lin, Z., Geng, S., Zhou, A., Zhang, W., Lu, P., He, C., Yue, X., Li, H., Qiao, Y.: Llama-adapter v2: Parameter-efficient visual instruction model. arXiv preprint arXiv:2304.15010 (2023)
- [21] Gao, P., Zhang, R., Liu, C., Qiu, L., Huang, S., Lin, W., Zhao, S., Geng, S., Lin, Z., Jin, P., et al.: Sphinx-x: Scaling data and parameters for a family of multi-modal large language models. arXiv preprint arXiv:2402.05935 (2024)
- [22] Gemini Team, G.: Gemini: a family of highly capable multimodal models. arXiv preprint arXiv:2312.11805 (2023)
- [23] Google: Bard (2023), <https://bard.google.com/>
- [24] Gou, Z., Shao, Z., Gong, Y., Yang, Y., Huang, M., Duan, N., Chen, W., et al.: Tora: A tool-integrated reasoning agent for mathematical problem solving. arXiv preprint arXiv:2309.17452 (2023)
- [25] Guo, Z., Zhang, R., Zhu, X., Tang, Y., Ma, X., Han, J., Chen, K., Gao, P., Li, X., Li, H., et al.: Point-bind & point-llm: Aligning point cloud with multi-modality for 3d understanding, generation, and instruction following. arXiv preprint arXiv:2309.00615 (2023)
- [26] Han, J., Zhang, R., Shao, W., Gao, P., Xu, P., Xiao, H., Zhang, K., Liu, C., Wen, S., Guo, Z., et al.: Imagebind-llm: Multi-modality instruction tuning. arXiv preprint arXiv:2309.03905 (2023)
- [27] Hu, E.J., Shen, Y., Wallis, P., Allen-Zhu, Z., Li, Y., Wang, S., Wang, L., Chen, W.: Lora: Low-rank adaptation of large language models. arXiv preprint arXiv:2106.09685 (2021)
- [28] Jiang, A.Q., Sablayrolles, A., Roux, A., Mensch, A., Savary, B., Bamford, C., Chaplot, D.S., de Las Casas, D., Hanna, E.B., Bressand, F., Lengyel, G., Bour, G., Lample, G., Lavaud, L.R., Saulnier, L., Lachaux, M., Stock, P., Subramanian, S., Yang, S., Antoniak, S., Scao, T.L., Gervet, T., Lavril, T., Wang, T., Lacroix, T., Sayed, W.E.: Mixtral of experts. Arxiv 2401.04088 (2024)
- [29] Jin, B., Zheng, Y., Li, P., Li, W., Zheng, Y., Hu, S., Liu, X., Zhu, J., Yan, Z., Sun, H., et al.: Tod3cap: Towards 3d dense captioning in outdoor scenes. arXiv preprint arXiv:2403.19589 (2024)
- [30] Kazemi, M., Alvari, H., Anand, A., Wu, J., Chen, X., Soricute, R.: Geomverse: A systematic evaluation of large models for geometric reasoning. arXiv preprint arXiv:2312.12241 (2023)

- [31] Li, B., Zhang, K., Zhang, H., Guo, D., Zhang, R., Li, F., Zhang, Y., Liu, Z., Li, C.: Llava-next: Stronger llms supercharge multimodal capabilities in the wild (May 2024), <https://llava-vl.github.io/blog/2024-05-10-llava-next-stronger-llms/>
- [32] Li, F., Zhang, R., Zhang, H., Zhang, Y., Li, B., Li, W., Ma, Z., Li, C.: Llava-next-interleave: Tackling multi-image, video, and 3d in large multimodal models (2024), <https://arxiv.org/abs/2407.07895>
- [33] Li, F., Zhang, R., Zhang, H., Zhang, Y., Li, B., Li, W., Ma, Z., Li, C.: Llava-next: Tackling multi-image, video, and 3d in large multimodal models (June 2024), <https://llava-vl.github.io/blog/2024-06-16-llava-next-interleave/>
- [34] Li, J., Li, D., Xiong, C., Hoi, S.: Blip: Bootstrapping language-image pre-training for unified vision-language understanding and generation. In: International Conference on Machine Learning. pp. 12888–12900. PMLR (2022)
- [35] Li, K., He, Y., Wang, Y., Li, Y., Wang, W., Luo, P., Wang, Y., Wang, L., Qiao, Y.: Videochat: Chat-centric video understanding. arXiv preprint arXiv:2305.06355 (2023)
- [36] Li, X., Zhang, M., Geng, Y., Geng, H., Long, Y., Shen, Y., Zhang, R., Liu, J., Dong, H.: Manipllm: Embodied multimodal large language model for object-centric robotic manipulation. arXiv preprint arXiv:2312.16217 (2023)
- [37] Liang, Z., Yang, T., Zhang, J., Zhang, X.: Unimath: A foundational and multimodal mathematical reasoner. In: EMNLP (2023)
- [38] Lin, Z., Liu, C., Zhang, R., Gao, P., Qiu, L., Xiao, H., Qiu, H., Lin, C., Shao, W., Chen, K., et al.: Sphinx: The joint mixing of weights, tasks, and visual embeddings for multi-modal large language models. arXiv preprint arXiv:2311.07575 (2023)
- [39] Liu, H., Li, C., Li, Y., Lee, Y.J.: Improved baselines with visual instruction tuning (2023)
- [40] Liu, H., Li, C., Li, Y., Li, B., Zhang, Y., Shen, S., Lee, Y.J.: Llava-next: Improved reasoning, ocr, and world knowledge (January 2024), <https://llava-vl.github.io/blog/2024-01-30-llava-next/>
- [41] Liu, H., Li, C., Wu, Q., Lee, Y.J.: Visual instruction tuning. In: NeurIPS (2023)
- [42] Liu, J., Li, C., Wang, G., Lee, L., Zhou, K., Chen, S., Xiong, C., Ge, J., Zhang, R., Zhang, S.: Self-corrected multimodal large language model for end-to-end robot manipulation. arXiv preprint arXiv:2405.17418 (2024)
- [43] Lu, P., Bansal, H., Xia, T., Liu, J., Yue Li, C., Hajishirzi, H., Cheng, H., Chang, K.W., Galley, M., Gao, J.: Mathvista: Evaluating math reasoning in visual contexts with gpt-4v, bard, and other large multimodal models. ArXiv **abs/2310.02255** (2023)
- [44] Lu, P., Gong, R., Jiang, S., Qiu, L., Huang, S., Liang, X., Zhu, S.C.: Inter-gps: Interpretable geometry problem solving with formal language and symbolic reasoning. arXiv preprint arXiv:2105.04165 (2021)
- [45] Ning, M., Wang, Q.F., Huang, K., Huang, X.: A symbolic characters aware model for solving geometry problems. In: Proceedings of the 31st ACM International Conference on Multimedia. p. 7767–7775. MM '23, Association for Computing Machinery, New York, NY, USA (2023). <https://doi.org/10.1145/3581783.3612570>, <https://doi.org/10.1145/3581783.3612570>
- [46] Nye, M., Andreassen, A.J., Gur-Ari, G., Michalewski, H., Austin, J., Bieber, D., Dohan, D., Lewkowycz, A., Bosma, M., Luan, D., et al.: Show your work: Scratchpads for intermediate computation with language models. arXiv preprint arXiv:2112.00114 (2021)
- [47] OpenAI: Chatgpt. <https://chat.openai.com> (2023)
- [48] OpenAI: Gpt-4 technical report. ArXiv **abs/2303.08774** (2023)
- [49] OpenAI: GPT-4V(ision) system card (2023), <https://openai.com/research/gpt-4v-system-card>

- [50] Ouyang, L., Wu, J., Jiang, X., Almeida, D., Wainwright, C., Mishkin, P., Zhang, C., Agarwal, S., Slama, K., Gray, A., Schulman, J., Hilton, J., Kelton, F., Miller, L., Simens, M., Askell, A., Welinder, P., Christiano, P., Leike, J., Lowe, R.: Training language models to follow instructions with human feedback. In: *Advances in Neural Information Processing Systems* (2022)
- [51] Radford, A., Kim, J.W., Hallacy, C., Ramesh, A., Goh, G., Agarwal, S., Sastry, G., Askell, A., Mishkin, P., Clark, J., Krueger, G., Sutskever, I.: Learning transferable visual models from natural language supervision. In: *International Conference on Machine Learning* (2021), <https://api.semanticscholar.org/CorpusID:231591445>
- [52] Shi, W., Hu, Z., Bin, Y., Liu, J., Yang, Y., Ng, S.K., Bing, L., Lee, R.K.W.: Math-llava: Bootstrapping mathematical reasoning for multimodal large language models. *arXiv preprint arXiv:2406.17294* (2024)
- [53] Shu, C., Chen, B., Liu, F., Fu, Z., Shareghi, E., Collier, N.: Visual med-llm: A parameter-efficient biomedical llm with visual capabilities (2023)
- [54] Singhal, K., Tu, T., Gottweis, J., Sayres, R., Wulczyn, E., Hou, L., Clark, K., Pfohl, S., Cole-Lewis, H., Neal, D., et al.: Towards expert-level medical question answering with large language models. *arXiv preprint arXiv:2305.09617* (2023)
- [55] Su, Y., Lan, T., Li, H., Xu, J., Wang, Y., Cai, D.: Pandagpt: One model to instruction-follow them all. *arXiv preprint arXiv:2305.16355* (2023)
- [56] Team, I.: Internlm: A multilingual language model with progressively enhanced capabilities (2023)
- [57] Team, Q.: Introducing qwen1.5 (February 2024), <https://qwenlm.github.io/blog/qwen1.5/>
- [58] Touvron, H., Lavril, T., Izacard, G., Martinet, X., Lachaux, M.A., Lacroix, T., Rozière, B., Goyal, N., Hambro, E., Azhar, F., et al.: Llama: Open and efficient foundation language models. *arXiv preprint arXiv:2302.13971* (2023)
- [59] Touvron, H., Martin, L., Stone, K., Albert, P., Almahairi, A., Babaei, Y., Bashlykov, N., Batra, S., Bhargava, P., Bhosale, S., et al.: Llama 2: Open foundation and fine-tuned chat models. *arXiv preprint arXiv:2307.09288* (2023)
- [60] Wang, K., Ren, H., Zhou, A., Lu, Z., Luo, S., Shi, W., Zhang, R., Song, L., Zhan, M., Li, H.: Mathcoder: Seamless code integration in LLMs for enhanced mathematical reasoning. In: *The Twelfth International Conference on Learning Representations* (2024), <https://openreview.net/forum?id=z8TW0ttBPp>
- [61] Wei, J., Wang, X., Schuurmans, D., Bosma, M., Xia, F., Chi, E., Le, Q.V., Zhou, D., et al.: Chain-of-thought prompting elicits reasoning in large language models. *Advances in Neural Information Processing Systems* **35**, 24824–24837 (2022)
- [62] Xu, R., Wang, X., Wang, T., Chen, Y., Pang, J., Lin, D.: Pointllm: Empowering large language models to understand point clouds. *arXiv preprint arXiv:2308.16911* (2023)
- [63] Yang, S., Liu, J., Zhang, R., Pan, M., Guo, Z., Li, X., Chen, Z., Gao, P., Guo, Y., Zhang, S.: Lidar-llm: Exploring the potential of large language models for 3d lidar understanding. *arXiv preprint arXiv:2312.14074* (2023)
- [64] Ye, Q., Xu, H., Xu, G., Ye, J., Yan, M., Zhou, Y., Wang, J., Hu, A., Shi, P., Shi, Y., Jiang, C., Li, C., Xu, Y., Chen, H., Tian, J., Qian, Q., Zhang, J., Huang, F.: mplug-owl: Modularization empowers large language models with multimodality (2023)
- [65] Ye, Q., Xu, H., Ye, J., Yan, M., Hu, A., Liu, H., Qian, Q., Zhang, J., Huang, F., Zhou, J.: mplug-owl2: Revolutionizing multi-modal large language model with modality collaboration (2023)
- [66] Yu, L., Jiang, W., Shi, H., Yu, J., Liu, Z., Zhang, Y., Kwok, J.T., Li, Z., Weller, A., Liu, W.: Metamath: Bootstrap your own mathematical questions for large language models. *arXiv preprint arXiv:2309.12284* (2023)

- [67] Yue, X., Qu, X., Zhang, G., Fu, Y., Huang, W., Sun, H., Su, Y., Chen, W.: Mammoth: Building math generalist models through hybrid instruction tuning. arXiv preprint arXiv:2309.05653 (2023)
- [68] Yue, X., Zheng, T., Zhang, G., Chen, W.: Mammoth2: Scaling instructions from the web. arXiv preprint arXiv:2405.03548 (2024)
- [69] Zhang, H., Chen, J., Jiang, F., Yu, F., Chen, Z., Li, J., Chen, G., Wu, X., Zhang, Z., Xiao, Q., et al.: Huatuogpt, towards taming language model to be a doctor. arXiv preprint arXiv:2305.15075 (2023)
- [70] Zhang, R., Han, J., Zhou, A., Hu, X., Yan, S., Lu, P., Li, H., Gao, P., Qiao, Y.: LLaMA-adapter: Efficient fine-tuning of large language models with zero-initialized attention. In: The Twelfth International Conference on Learning Representations (2024), <https://openreview.net/forum?id=d4UiXAHN2W>
- [71] Zhang, R., Jiang, D., Zhang, Y., Lin, H., Guo, Z., Qiu, P., Zhou, A., Lu, P., Chang, K.W., Gao, P., et al.: Mathverse: Does your multi-modal llm truly see the diagrams in visual math problems? arXiv preprint arXiv:2403.14624 (2024)
- [72] Zhou, A., Wang, K., Lu, Z., Shi, W., Luo, S., Qin, Z., Lu, S., Jia, A., Song, L., Zhan, M., et al.: Solving challenging math word problems using gpt-4 code interpreter with code-based self-verification. arXiv preprint arXiv:2308.07921 (2023)

A Appendix

A.1 Details of Mathematical Visual Dataset

A.1.1 Data Engine

In this section, we detail the implementation specifics of our data engine, i.e., the process for generating diagrams related to plane geometry, analytic geometry, and function domains.

Plane Geometry Diagram. Inspired by previous multi-hop reasoning methods [30, 61, 46], we employ an iterative generation method over logical theories to generate plane geometric images along with corresponding captions and question-answering pairs, whose complexity can be controlled across multiple axes. Specifically, we first define a set of fundamental geometric shapes in Figure 5.

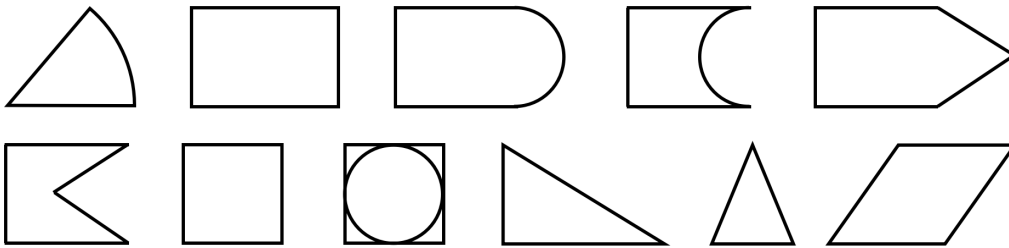


Figure 5: The set of fundamental shapes in plane geometry diagrams, whose straight edges can be extended into other basic shapes.

Within each shape, new basic shapes can be generated by extending a particular edge. For each basic shape, we initially define a meta reasoning process:

$$O_{n-1}, C_{m_{n-1}}^i \xrightarrow{E_{m_{n-1}}^i} O_n, i \in [1, z], \quad (1)$$

where O represents the initial side length of the shape, C_m denotes the additional conditions required to complete meta reasoning, and E_m provides a detailed explanation of the meta reasoning process. For example, when considering an isosceles triangle as the $(n-1)^{th}$ shape in a sequence, the vertex angle is still required as C_m to reason about base side length, and then to expand to the n^{th} shape,

with E_m serving as the explanation of this process. The variable z indicates that there are z sets of possible meta reasoning for the shape, n indicates the length of the generating sequence, which is also the number of hops of reasoning required to answer the question. The initial side, extend side, and additional conditions for meta-reasoning of each basic shape can be referred to in Fig.5. In the final shape, question-answering pairs pertinent to this shape can be generated as

$$O_n, C_{q_n}^j, Q_n^j \xrightarrow{E_{q_n}^j} A_n^j, j \in [1, m], \quad (2)$$

where C_q represents the additional conditions required to solve the problem, while Q and A denote the question and answer, respectively. E_q refers to the detailed explanation of the solving process. The variable m indicates that there are m pairs of question-answering and corresponding detailed explanations within the shape. By applying meta reasoning to the $n - 1$ th shape, the initial side length of the n th shape can be deduced. Therefore, for a complex composite figure consisting of n shapes, the overall question-answering pair can be defined as follows:

$$O_1, \sum_{k=1}^{n-1} C_{m_k}^j, C_{q_n}^j, Q_n^j \xrightarrow{E_{q_n}^j} A_n^j. \quad (3)$$

Each shape defines a sufficient number of conditions, explanations, and answers to ensure the diversity of the generated question-answering pairs. Based on the aforementioned rules, controlling the length of the generation sequence can regulate the number of reasoning steps, and controlling the type of questions can manage the knowledge required for solving the problems. Thus, we can generate questions of varying difficulty levels. The aforementioned generation process can also be illustrated in Figure 7.

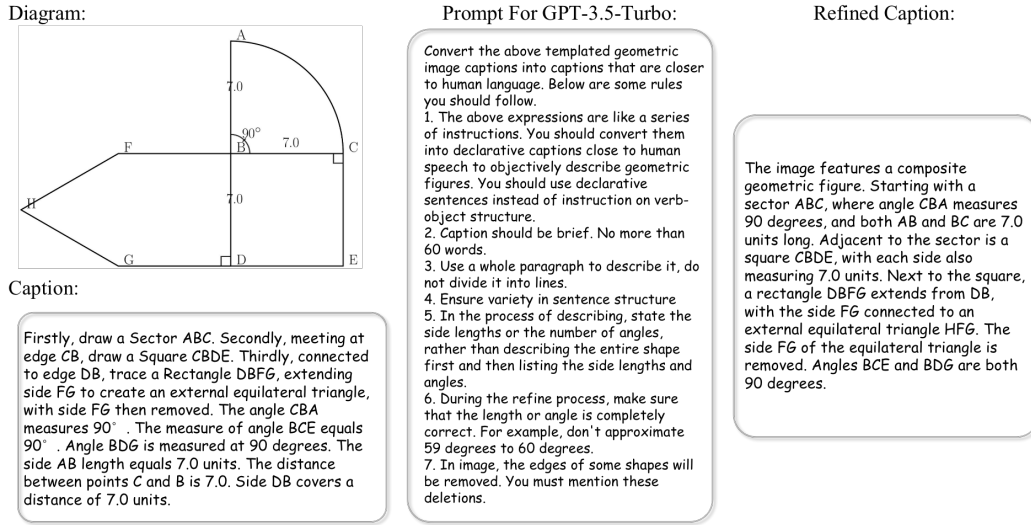


Figure 6: Plain geometry caption examples.

Analytic Geometry Diagram. The image generation method for analytic geometry is relatively straightforward. First, we randomly select a range within the coordinate system: the minimum value of x is chosen as an integer between $[-12, -8]$, and the maximum value of x is chosen as an integer between $[8, 12]$; the range for y is the same as for x . Then, we define the following basic shapes: point, line segment, line, circle, ellipse, rectangle, square, polygon, and sector. During the generation process, we select a number between 1 and 4 as the number of shapes to generate. The generation rule is that **nonlinear shapes** other than points, line segments, and lines **must not overlap**.

Function Diagram. The generation of function graphs is also straightforward. We define the following basic functions, each with a set of parameters that can be randomly selected:

Sine Function $y = A \cdot \sin(f \cdot x + \phi)$, where the amplitude A is a random integer between 1 and 3, the frequency f is either 1 or 2, and the phase ϕ is a random integer between 0 and 2π .

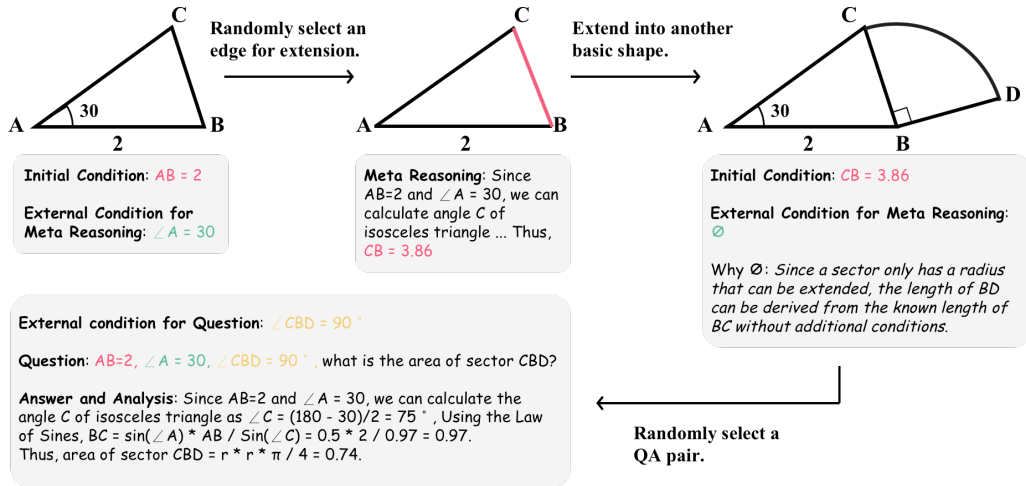


Figure 7: A single process for generating plane geometry diagrams and corresponding question-answering pairs is described. In this example, the generation sequence length is specified as 2. **Initial side length** is painted as pink, C_m is painted as green, while C_q is painted as yellow.

Cosine Function	$y = A \cdot \cos(f \cdot x + \phi)$, where the amplitude A is a random integer between 1 and 3, the frequency f is either 1 or 2, and the phase ϕ is a random integer between 0 and 2π .
Tangent Function	$y = A \cdot \tan(f \cdot x + \phi)$, where the amplitude A is a random integer between 1 and 3, the frequency f is either 1 or 2, and the phase ϕ is a random integer between 0 and 2π .
Polynomial Function	$P(x) = a_n x^n + a_{n-1} x^{n-1} + \dots + a_1 x + a_0$, where the degree n is a random integer between 1 and 4. The coefficients a_i are randomly selected integers ranging from -3 to 3.
piece-wise Function	piece-wise polynomial functions are divided into 2 or 3 segments, with each segment's parameters identical to those of a polynomial function.
Logarithmic Function	$y = a \cdot \log_b(c \cdot x + d)$, where the coefficient a is randomly chosen from $\{-3, -2, -1, 1, 2, 3\}$, the base b is randomly chosen from $\{2, 10, [e]\}$, the coefficient c is a random integer between 1 and 3, and the coefficient d is a random integer between 1 and 6, ensuring that $c \cdot x + d$ is positive.
Absolute Function	$y = a \cdot x + b $, where a and b are random integer between -5 and 5 .

We first determine the domain range to be displayed on the function graph. For trigonometric functions, the domain is set to $[-\pi, \pi]$. For piece-wise polynomial functions, the minimum value of x is a random integer between $[-12, -8]$, and the maximum value of x is a random integer between $[8, 12]$. For other functions, the minimum and maximum values of x are random integers within the ranges of $[-6, -3]$ and $[3, 6]$, respectively. During the plotting process, we calculate the local maxima, minima, and zeros of the function by iterating through the domain. We then render the x-coordinates of these extrema and zeros on the x-axis of the function graph.

A.1.2 MAVIS-Caption

In this section, we detail how the captions corresponding to images in the MAVIS-Caption Dataset are generated.

Plane Geometry Caption. Based on the generation process described in Section A.1.1, when generating each shape, a caption is randomly selected from a set of captions for that shape and some connecting words are randomly added. The captions for each shape can be referenced in Section ???. We also randomly select some edges or angles and state their measurements in the caption. After

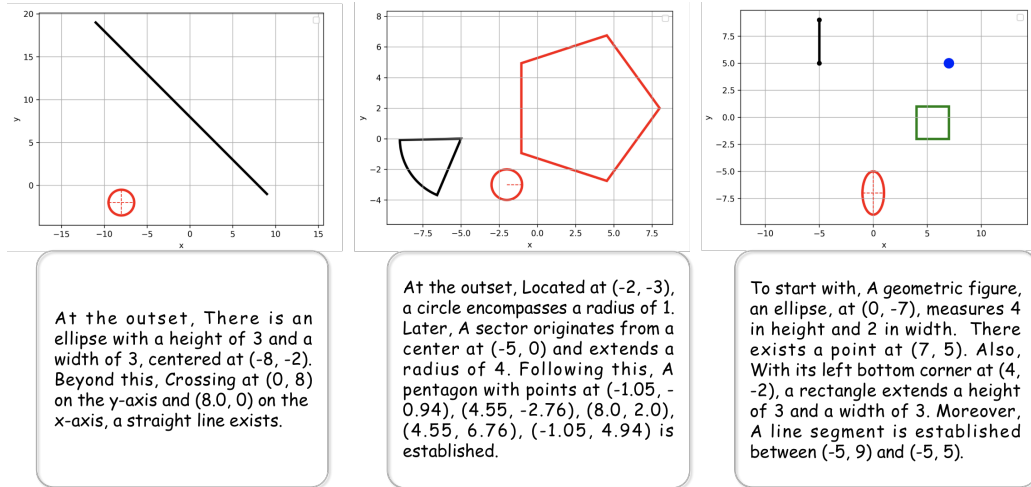


Figure 8: Examples of analytical geometry diagram caption.

generating the raw caption, we use GPT-3.5 to refine it, enhancing its linguistic structure and semantic diversity. An example is shown in Fig.6.

Analytic Geometry Caption. For each shape, we maintain a set of caption templates that describe the shape's type, coordinate position, and other attributes. Specific templates can be referenced in Section ???. In the generation process described in Section A.1.1, we select a template and randomly add some diverse connecting words to form a complete caption. Examples of some captions are shown in Fig.8.

Function Caption. According to the function graph generation process described in Section A.1.1, we record the function's zeros and extrema. Additionally, we also record the function's expression and asymptotes. These attributes are incorporated into a randomly selected caption template to form the function graph's caption. Caption templates can be referenced in Section ???. Some examples are provided in Fig.9.

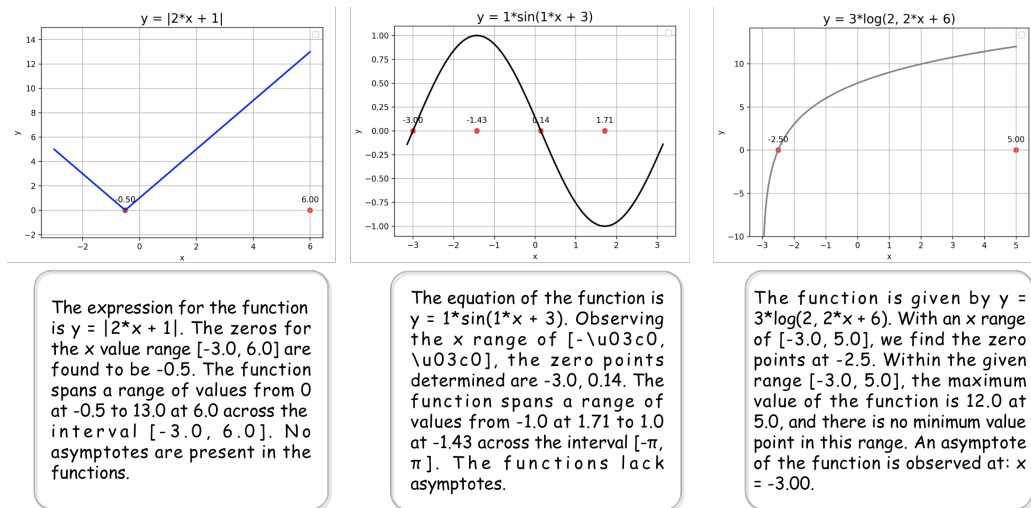


Figure 9: Function diagram captions.

A.1.3 MAVIS-Instruct

Manual Collection Augmented by GPT-4. To complement the dataset with real-world problem-solving scenarios, we hire 8 human experts to manually collect visual math problems from various

public sources^{1,2,3}, spanning plane geometry, analytic geometry, and function. For problems, we try to obtain their content as complete as possible, including questions, diagrams, answers, and rationales if available. Then, we first feed all the related information into GPT-4V to eliminate the redundant information within text questions, constructing the text-lite version of problems by the prompt in Figure 10. Then, we design three types of prompts for GPT-4 to augment 15 multiple-choice questions (including 10 multiple-choice and 5 binary-choice, i.e., ‘True’ or ‘False’) and 5 free-form questions, respectively, as shown in Figure 11. We do not adopt GPT-4V here, since GPT-4V itself would misunderstand diagrams for low-quality data augmentation. The newly generated problems contain detailed CoT rationales and diverse question forms.

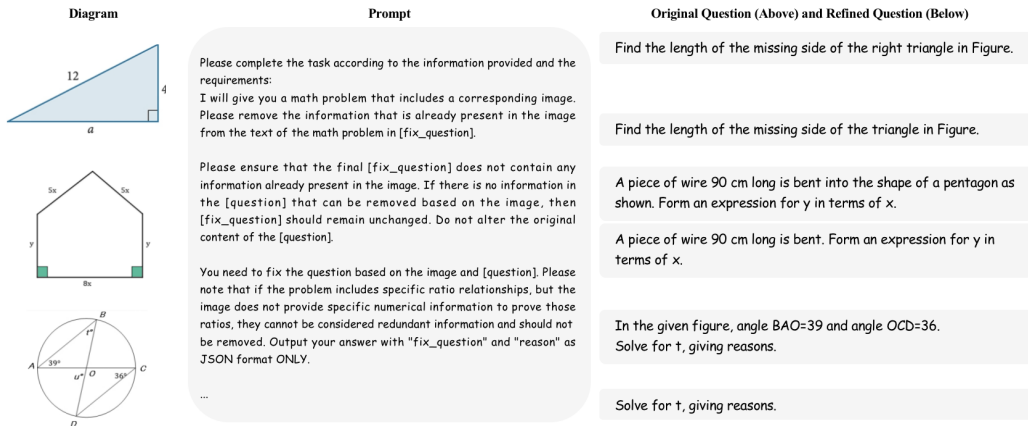


Figure 10: Manually collect visual math problems text-lite version.

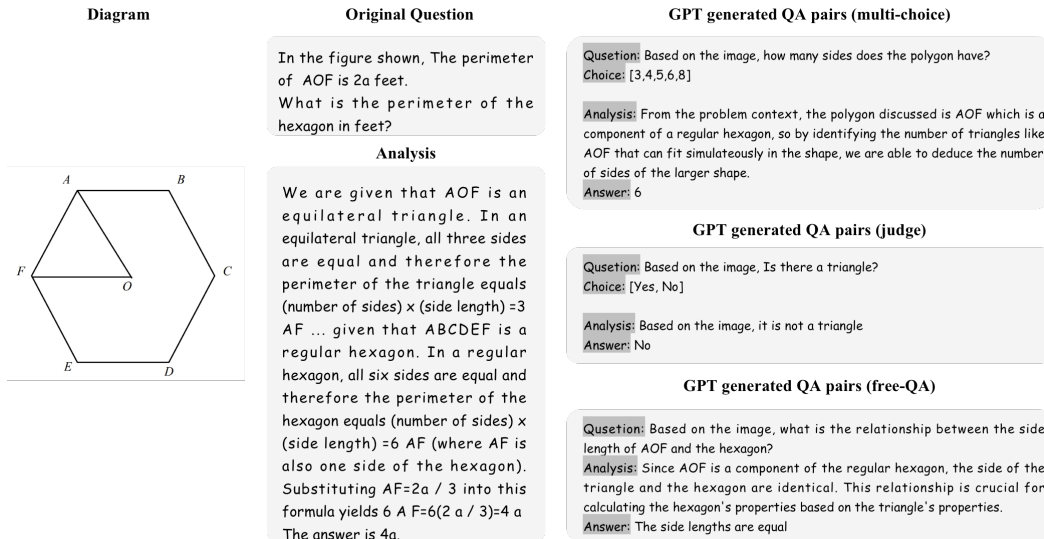


Figure 11: We design different types of prompts for GPT-4 to augment 15 multiple-choice questions and 5 free-form questions, respectively.

Existing Datasets Augmented by GPT-4. Previous efforts have been made to provide some small-scale, plane geometry datasets, e.g., GeoQA [12], GeoQA+ [10], and Geometry3K [44]. Although they are limited in data scale for tuning MLLMs and include no rationales, we can also regard them as a seed dataset and adopt GPT-4 to augment larger-scale training data. We do not utilize GPT-4V here for the

¹<https://homework.study.com>

²<https://www.ixl.com/math>

³<https://mathspace.co/us>

same reason aforementioned. In detail, we design 3 types of question generation approaches using different prompts, as shown in Fig. 12. For Geometry3K, as the question texts are normally brief and contain marginal descriptive information, posing challenges for GPT-4 to understand the diagram, we only augment them to generate binary-choice questions, i.e., ‘True’ or ‘False’. For GeoQA+, we can leverage the sufficient redundant information within their texts to generate more diverse and accurate multi-choice and free-form questions. Likewise, GPT-4 can produce CoT rationales for each problem.

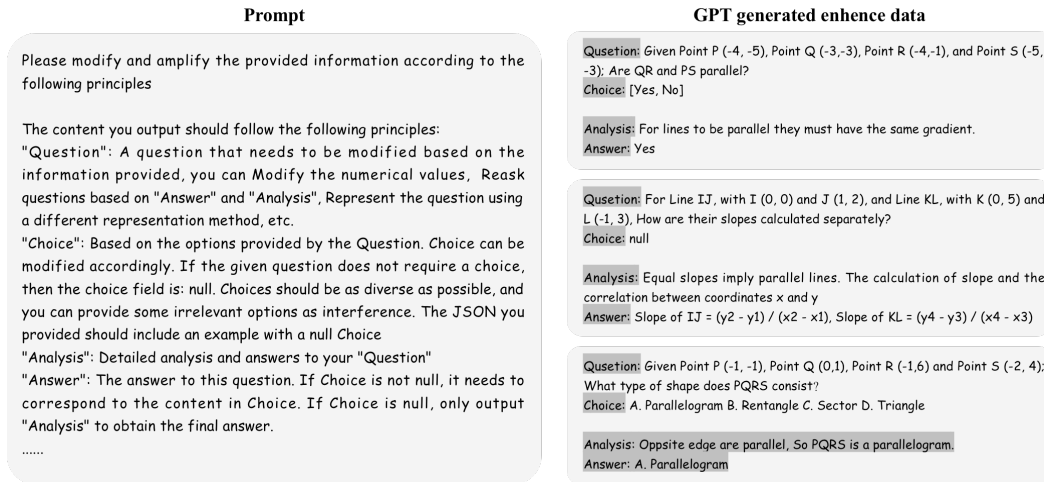


Figure 12: We design 3 types of question generation approaches using different prompts to augment existing visual mathematical dataset.

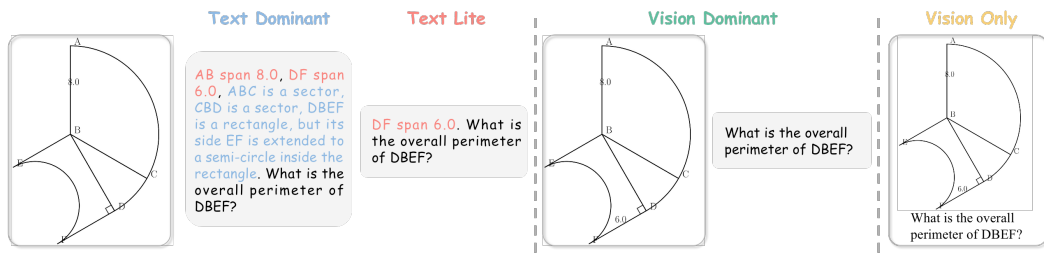


Figure 13: The Text Dominant, Text Lite, Vision Dominant, and Vision Only versions of the same question. Text Dominant and Text Lite use the same image. In the text, the necessary conditions for solving the problem are highlighted in red, while redundant descriptive conditions are highlighted in blue. In the Vision Only version, the question is rendered in the image, with no textual question provided.

Data Engine Captions Annotated by GPT-4.

Given the delicately designed data engine for automatic diagram-caption creation, we can utilize the generated large-scale pairs to annotate question-answering data using GPT-4V. Different from the previous two sources that augment questions based on questions, we utilize the GPT-4V model here for caution data with two reasons: first, the detailed caption from our data engine can well guide GPT-4V for relatively higher-quality visual embedding; second, the visual input serves as guidance to provide additional spatial information for broad question forms. As shown in Fig. 20 and Fig. 21, we adopt different prompts for function and plane geometry problems, ensuring that the generated question-answering data is of high quality for instruction tuning.

Data Engine Generated Problems.

Plane Geometry. Based on the generation process described in Section A.1.1, we pose questions about the final shape in the generation sequence. We designed 6 types of questions: finding the

perimeter

What is the perimeter of {shape_id}?
How long is the perimeter of {shape_id}?
What is the total length of the perimeter of {shape_id}?
Can you calculate the perimeter of {shape_id}?
How do you find the perimeter of {shape_id}?
What is the measurement of the perimeter of {shape_id}?
What is the total perimeter measurement of {shape_id}?
Could you determine the perimeter of {shape_id}?
What would the perimeter of {shape_id} be?
What is the perimeter length of {shape_id}?
How would you calculate the perimeter of {shape_id}?
What' s the perimeter of {shape_id}?
How much is the perimeter of {shape_id}?
Can you tell me the perimeter of {shape_id}?
What is the total boundary length of {shape_id}?
What is the entire perimeter length of {shape_id}?
How do you measure the perimeter of {shape_id}?
How would you determine the perimeter of {shape_id}?
What is the full perimeter of {shape_id}?
What is the overall perimeter of {shape_id}?
How can we calculate the perimeter of {shape_id}?

Figure 14: Perimeter problem templates.

area

What is the area of the entire shape {shape_id}?
How much is the area of the entire shape {shape_id}?
What is the total area of the shape {shape_id}?
Can you calculate the area of the entire shape {shape_id}?
What is the overall area of the shape {shape_id}?
How do you find the area of the entire shape {shape_id}?
What is the measurement of the total area of {shape_id}?
What is the total area measurement of the shape {shape_id}?
Could you determine the area of the entire shape {shape_id}?
What would the area of the entire shape {shape_id} be?
What is the area size of the entire shape {shape_id}?
How would you calculate the total area of the shape {shape_id}?
What' s the area of the entire shape {shape_id}?
How much area does the shape {shape_id} cover?
Can you tell me the area of the whole shape {shape_id}?
What is the overall area measurement of the shape {shape_id}?
What is the full area of the shape {shape_id}?
How do you calculate the area of the shape {shape_id}?
What is the total surface area of the shape {shape_id}?
How can we determine the area of the entire shape {shape_id}?
What is the total area of shape {shape_id}?

Figure 15: Area problem templates.

base length

What is the length of the base {base_side_id} in isosceles triangle {shape_id}?
Can you tell me the length of the base {base_side_id} in the isosceles triangle {shape_id}?
What is the measurement of the base {base_side_id} in the isosceles triangle {shape_id}?
How long is the base {base_side_id} in the isosceles triangle {shape_id}?
What is the base length {base_side_id} in the isosceles triangle {shape_id}?
Could you provide the length of the base {base_side_id} in the isosceles triangle {shape_id}?
Can you specify the length of the base {base_side_id} in the isosceles triangle {shape_id}?
I need to know the length of the base {base_side_id} in the isosceles triangle {shape_id}.
Please tell me the length of the base {base_side_id} in the isosceles triangle {shape_id}.
What is the length of the side {base_side_id} that forms the base of the isosceles triangle {shape_id}?

Figure 16: Base length problem templates.

perimeter, finding the area, finding the base length, finding the angle, finding the arc length, and finding the extended edge length. Each type of question has a set of templates that can be randomly selected, as shown in Figure 14-19. As for the answer and analysis, each shape has a set of templates for different types of questions to choose from, as shown in Sec.A.1.1.

To further enhance the model's understanding of different forms of questions and better utilize the diverse modal information in the text and images, we divided the plain geometry questions generated by the Data Engine into four versions referring to MathVerse [71]: Text Dominant, Text Lite, Vision Dominant, and Vision Only.

Text Dominant We marked all the conditions required for solving the problem in the diagram and also described these conditions in the text, along with some redundant descriptive text.

Text Lite All the conditions required for solving the problem are randomly divided into two parts: one part is marked in the diagram, and the other part is described in the text. In other words, the conditions in the diagram and the conditions in the text do not overlap.

Vision Dominant	All the conditions required for solving the problem are marked in the diagram, while the text only contains the question without any conditions.
Vision Only	Not only are all the conditions required for solving the problem marked in the diagram, but the question is also rendered in the diagram, leaving the text portion empty.

The differences among the four versions of the same question are illustrated in Figure 13. Each basic shape will retain a set of redundant conditions. During the shape generation process, there is a 50% probability of including these redundant conditions.

angle

- In isosceles triangle {shape_id}, what is the measure of angle {bottom_angle_0} and angle {bottom_angle_1}?
- In isosceles triangle {shape_id}, what is the measure of angle {bottom_angle_0} and angle {bottom_angle_1}?
- What are the measures of angle {bottom_angle_0} and angle {bottom_angle_1} in the isosceles triangle {shape_id}?
- Can you tell me the measures of angle {bottom_angle_0} and angle {bottom_angle_1} in the isosceles triangle {shape_id}?
- In the isosceles triangle {shape_id}, what are the measures of angle {bottom_angle_0} and angle {bottom_angle_1}?
- What is the measurement of angle {bottom_angle_0} and angle {bottom_angle_1} in the isosceles triangle {shape_id}?
- How large are angle {bottom_angle_0} and angle {bottom_angle_1} in the isosceles triangle {shape_id}?
- Please provide the measures of angle {bottom_angle_0} and angle {bottom_angle_1} in the isosceles triangle {shape_id}.
- What are the measures of angles {bottom_angle_0} and {bottom_angle_1} in the isosceles triangle {shape_id}?
- Can you specify the measures of angle {bottom_angle_0} and angle {bottom_angle_1} in the isosceles triangle {shape_id}?
- In the isosceles triangle {shape_id}, what are the measurements of angle {bottom_angle_0} and angle {bottom_angle_1}?

Figure 17: Angle problem templates.

arc length

- In sector {shape_id}, what is the length of arc {arc_id}?
- What is the length of arc {arc_id} in sector {shape_id}?
- Can you tell me the length of arc {arc_id} in sector {shape_id}?
- In the sector {shape_id}, what is the measurement of arc {arc_id}?
- How long is arc {arc_id} in sector {shape_id}?
- Please provide the length of arc {arc_id} in sector {shape_id}.
- What is the arc length {arc_id} in the sector {shape_id}?
- Could you specify the length of arc {arc_id} in sector {shape_id}?
- What is the measurement of arc {arc_id} in the sector {shape_id}?
- In sector {shape_id}, how long is arc {arc_id}?

Figure 18: Arc length problem templates.

extend side length

- In shape {shape_id}, what is the length of {extend_side_id}?
- What is the length of {extend_side_id} in shape {shape_id}?
- Can you tell me the length of {extend_side_id} in shape {shape_id}?
- In the shape {shape_id}, what is the measurement of {extend_side_id}?
- How long is {extend_side_id} in shape {shape_id}?
- Please provide the length of {extend_side_id} in shape {shape_id}.
- What is the side length {extend_side_id} in the shape {shape_id}?
- Could you specify the length of {extend_side_id} in shape {shape_id}?
- What is the measurement of {extend_side_id} in the shape {shape_id}?
- In shape {shape_id}, how long is {extend_side_id}?

Figure 19: Extend side length problem templates.

Diagram:

Caption:

The function can be described by the equation $y = 1 \cdot \cos(1 \cdot x + 3)$. With an x range of $[-\pi, \pi]$, we find the zero points at -1.43, 1.71. Exploring the function within the range $[-\pi, \pi]$, we find that the highest value it reaches is 1.0 at -3.0, and the lowest value is -1.0 at 0.14. There are no asymptotes in the functions.

Prompt for Function Problems:

Here is some more supplementary information for the diagram I give you: "(caption)"
Please first watch the diagram and ask a question that can be correctly answered only by seeing the diagram.
Then you should correctly analysis the question and give the answer.
The reasoning process should not use "According to the caption" or something like that.
Next, you should give 3 other hard false choices along with the correct one.

You should totally provide 3 questions.
The type of questions is multi-choice.

You should strictly follow this format and order (end every problem with #####):
QUESTION: What is the maximum value of the function in the given range?
ANSWER: B. 4
CHOICE: A. 3; B. 4; C. 2; D. 1 #####

Question & Rationale Generated by GPT-4V:

Question:
What is the length of square side FG? Choices: A. 10.0; B. 10.1; C. 9.9; D. 10.5

Rational:
Since FG is a side of square DCFG, and the properties of a square dictate that all sides are equal in length, the length of FG must be the same as DC which is given as 10.0 units. So the answer is A.

Question:
What is the length of diagonal AC in triangle ABC? Choices: A. 10.1; B. 9.8; C. 9.9; D. 10.0

Rational:
In right triangle ABC with sides AB = 7.0 and BC = 7.0 units, and angle ACB = 45°, the triangle is isosceles. The length of diagonal AC can be calculated using the Pythagorean theorem: $AC = \sqrt{(AB)^2 + (BC)^2} = \sqrt{(7.0)^2 + (7.0)^2} = \sqrt{98} = 9.9$. So the answer is C.

Question:
What is the perimeter of quadrilateral CBDE? Choices: A. 33.0; B. 34.0; C. 35.0; D. 32.0

Rational:
The perimeter of quadrilateral CBDE includes sides CB, BD, DE, and EC. Given CB = 7.0, BD = 10.0, and knowing quadrilateral CBDE has parallel and equal opposite sides, DE = CB and EC = BD. Thus, DE = 7.0 and EC = 10.0. The perimeter = CB + BD + DE + EC = 7.0 + 10.0 + 7.0 + 10.0 = 34.0 units. So the answer is B.

Figure 20: The function prompt for GPT-4V and the generated questions and rationals.

Diagram:

Caption:

Firstly, trace a Right Triangle ABC. Secondly, attached to edge CB, draw a Quadrilateral with opposite sides parallel and equal in length CBDE. Thirdly, joined to edge DB, render a Square DCFG. The measurement of angle ACB is 45°. The angle DBC measures 60°. Angle BDG measures 90° in size. The distance between points A and G is 7.0. The segment CB spans 7.0 units. Side DB spans 10.0 units.

Prompt for Plane Geometry Problems:

Here is some more supplementary information of the diagram I give you: "(caption)"
Please first watch the diagram and ask a question that can be correctly answered only by seeing the diagram.
Then you should correctly analysis the question and give the answer.
The reasoning process should not use "According to the caption" or something like that.
Next, you should give 3 other hard false choices along with the correct one.

You should totally provide 3 questions.
The type of questions is multi-choice.

You should strictly follow this format and order (end every problem with #####):
QUESTION: What is the height of the trapezium ABCD?
ANSWER: B. 11.7
CHOICE: A. 11; B. 11.7; C. 12; D. 8 #####

Question & Rationale Generated by GPT-4V:

Question:
What is the length of square side FG? Choices: A. 10.0; B. 10.1; C. 9.9; D. 10.5

Rational:
Since FG is a side of square DCFG, and the properties of a square dictate that all sides are equal in length, the length of FG must be the same as DC which is given as 10.0 units. So the answer is A.

Question:
What is the length of diagonal AC in triangle ABC? Choices: A. 10.1; B. 9.8; C. 9.9; D. 10.0

Rational:
In right triangle ABC with sides AB = 7.0 and BC = 7.0 units, and angle ACB = 45°, the triangle is isosceles. The length of diagonal AC can be calculated using the Pythagorean theorem: $AC = \sqrt{(AB)^2 + (BC)^2} = \sqrt{(7.0)^2 + (7.0)^2} = \sqrt{98} = 9.9$. So the answer is C.

Question:
What is the perimeter of quadrilateral CBDE? Choices: A. 33.0; B. 34.0; C. 35.0; D. 32.0

Rational:
The perimeter of quadrilateral CBDE includes sides CB, BD, DE, and EC. Given CB = 7.0, BD = 10.0, and knowing quadrilateral CBDE has parallel and equal opposite sides, DE = CB and EC = BD. Thus, DE = 7.0 and EC = 10.0. The perimeter = CB + BD + DE + EC = 7.0 + 10.0 + 7.0 + 10.0 = 34.0 units. So the answer is B.

Figure 21: The geometry prompt for GPT-4V and the generated questions and rationals.

Function. All functions will be examined with two types of questions: finding the derivative and finding the extrema. After obtaining the derivative, we calculate whether the derivative has zeros within the given domain. The presence of zeros determines the method for calculating the function's extrema.

	Initial Side	Extend Side	Additional Condition for Meta Reasoning
	AB	BC	\emptyset
	AB	CD	\emptyset
	AB	\emptyset	
	AB	\emptyset	
	AB	CE DE	CDE is a equilateral triangle
	AB	\emptyset	
	AB	AD CD BC	\emptyset
	AB	AD BC CD	\emptyset
	AB	CD	\emptyset
	AB	AC BC	$\angle C = x \text{ degree}$
	AB	AC BC	$\angle B = x \text{ degree}$

Figure 22: The initial side, extend side, and additional conditions for meta-reasoning of each basic shape. Some special shapes are not extended and only appear in the last position of the generation sequence, thus their extend side is \emptyset .